NeuroImage xxx (2011) xxx–xxx

Contents lists available at ScienceDirect

NeuroImage

journal homepage: www.elsevier.com/locate/ynimg

Structural MRI detects progressive regional brain atrophy and neuroprotective effects in N171-82Q Huntington's disease mouse model

Yong Cheng [a,1], Qi Peng [a,1], Zhipeng Hou [b,1], Manisha Aggarwal [b], Jiangyang Zhang [b], Susumu Mori [b,g], Christopher A. Ross [a,c,d,e,f], Wenzhen Duan [a,f,*]

[a] Division of Neurobiology, Department of Psychiatry and Behavioral Sciences, Johns Hopkins University School of Medicine, Baltimore, MD 21287, USA
[b] Department of Radiology, Johns Hopkins University School of Medicine, Baltimore, MD 21287, USA
[c] Department of Neuroscience, Johns Hopkins University School of Medicine, Baltimore, MD 21287, USA
[d] Department of Neurology, Johns Hopkins University School of Medicine, Baltimore, MD 21287, USA
[e] Department of Pharmacology and Molecular Sciences, Johns Hopkins University School of Medicine, Baltimore, MD 21287, USA
[f] Program in Cellular and Molecular Medicine, Johns Hopkins University School of Medicine, Baltimore, MD 21287, USA
[g] F.M. Kirby Functional Imaging Center, Kennedy Krieger Institute, Baltimore, MD 21205, USA

ARTICLE INFO

Article history:
Received 7 November 2010
Revised 31 January 2011
Accepted 7 February 2011
Available online xxxx

Keywords:
Huntington's disease
MRI
LDDMM
Brain atrophy
Biomarker
SSRI

ABSTRACT

Huntington's disease (HD) displays progressive striatal atrophy that occurs long before the onset of clinical motor symptoms. As there is no treatment for the disease once overt symptoms appear, it has been suggested that neuroprotective therapy given during this presymptomatic period might slow progression of the disease. This requires biomarkers that can reliably detect early changes and are sensitive to treatment response. In mouse models of HD, structural MRI measures have been shown to detect disease onset. To determine whether such measures could also be suitable biomarkers for following responses to treatment, we used T2-weighted MR imaging combined with automated morphological analyses and characterized changes in regional brain volumes longitudinally in the N171-82Q HD mouse model in a preclinical trial. We report here that N171-82Q HD mice exhibit adult-onset and progressive brain atrophy in the striatum and neocortex as well as in whole brain; the progressive atrophy in striatum and neocortex is positively correlated with motor deficits. Most notably, MRI also detected neuroprotective effects of sertraline treatment, a neuroprotective agent confirmed in our previous studies. Our present studies provide the first evidence that longitudinal structural MRI measures can detect the therapeutic effect in HD mice, suggesting that such measures in brain could be valuable biomarkers in HD clinical trials.

Introduction

Huntington's disease (HD) is a dominantly inherited neurodegenerative disorder in which an expanded CAG triplet on the gene huntingtin has shown full penetrance; it is characterized by progressive impairment of motor function, psychiatric disturbance and dementia. The earliest and most striking neuropathological changes are atrophy occurring in the striatum (Halliday et al., 1998). More widespread neurodegeneration is also detected in other brain regions comprising both gray matter and white matter (Hobbs et al., 2010a,b; Rosas et al., 2010, 2006; Reading et al., 2005; Ciarmiello et al., 2006). Changes in brain volumes can precede overt symptoms by many years in HD (Hobbs et al., 2010a,b; Nopoulos et al., 2010; Wild et al., 2010; Aylward et al., 2000; Paulsen et al., 2008). Therefore, in HD treatment trials, it is important to determine not only the efficacy of the treatment but also when the treatment should begin, because neuroprotective therapy might provide stronger benefits if given before overt clinical symptoms. The challenge is to evaluate putative neuroprotection before the onset of clinical symptoms; thus, development of biomarkers with which the changes could be detected in the presymptomatic stage could be extremely valuable for the assessment of neuroprotective therapies in HD.

MRI-based measurement is a potential candidate for assessing regional volumetric change and it has been associated with known pathology of HD. Studies suggest that clinical trial of a putative neuroprotective agent could begin as early as 15 years prior to estimated motor diagnosis in a cohort of persons at risk for, but not meeting clinical motor diagnostic criteria for HD, and that neuroimaging might be among the best predictors of early diagnosis (Nopoulos et al., 2010; Paulsen et al., 2010; Rosas et al., 2010; Tabrizi et al., 2009). Validation of MRI-based volumetric measures as biomarkers should be done longitudinally to determine when the specific brain region first shows detectable atrophy, whether the degree of atrophy correlates with disease progression, how progression of brain atrophy correlates with other detectable

* Corresponding author at: Division of Neurobiology, Department of Psychiatry, Johns Hopkins University School of Medicine, CMSC 8-121, 600 N. Wolfe Street, Baltimore, MD 21287, USA. Fax: +1 410 614 0013.
E-mail address: wduan2@jhmi.edu (W. Duan).
[1] These authors contributed equally to this work.

1053-8119/$ – see front matter © 2011 Elsevier Inc. All rights reserved.
doi:10.1016/j.neuroimage.2011.02.022

phenotypes, and most importantly, how the brain atrophy responds to treatment.

Structural MRI measures of striatal volume changes may be sensitive and reliable for early disease detection and serve as a biomarker for HD. Indeed, there is a wealth of evidence that striatal atrophy can be detected by MRI up to 23 years prior to predicted motor onset, that striatal volume is negatively correlated with motor function and CAG repeat length, and that striatum continues to shrink with disease progression (Harris et al., 1992, 1996, 1999; Aylward et al., 1997, 2004; Rosas et al., 2001; Kassubek et al., 2004; Paulsen et al., 2006). More recent studies indicated that structural MRI can detect early brain volume changes (Nopoulos et al., 2010; Paulsen et al., 2010, 2008; Kloppel et al., 2009; Tabrizi et al., 2009), but whether it has adequate sensitivity to assess the outcome of neuroprotective trials remains unknown. Use of MRI measures as biomarkers for clinical therapeutic trials requires validation.

HD mouse models provide a unique model system with which to validate the imaging measures as biomarkers. Among available HD mouse models, fragment HD models, R6/2 and N171-82Q models, are most widely used in preclinical trials, as these mice display multiple phenotypic changes and brain pathology resembling those in HD patients; whereas full-length HD moue models often have subtle phenotypic changes, making it less feasible to use them in short preclinical trials. It was reported that structural MRI combined with voxel-based morphometry showed brain atrophy in cross-sectional studies of R6/2 mice (Sawiak et al., 2009a,b). We further characterized brain volumetric changes longitudinally in R6/2 mice (Zhang et al., 2010). Our results indicate that R6/2 model displayed detectable brain atrophy at 3 weeks of age, and it was difficult to track disease onset for use in presymptomatic trials. Therefore, we turned to the N171-82Q mouse model, that showed adult-onset behavioral deficits and other phenotypic changes that are less aggressive than those in R6/2 mice, suggesting that N171-82Q model might be suitable for both presymptomatic and symptomatic preclinical trials. We chose sertraline, a selective serotonin reuptake inhibitor (SSRI), as our positive drug to determine the sensitivity of structural MRI measures, as we have demonstrated that sertraline has neuroprotective effects in HD mice by increasing brain-derived neurotrophic factor and neurogenesis and that it attenuated brain atrophy in HD mice as indicated by histological analysis (Duan et al., 2008; Peng et al., 2008).

We used T2-weighted structural MRI combined with automated deformation-based morphometry analysis to characterize regional brain volume changes, correlate with other HD-like phenotypes, and evaluate the therapeutic response to a neuroprotective agent in the N171-82Q HD model. We found that N171-82Q HD mice exhibited adult-onset brain regional atrophy, that the atrophy is progressive, and most importantly, that MRI could detect the therapeutic response in these mice. Our current findings provide to our knowledge the first evidence that structural MRI could detect treatment response, and provide proof-of-principle for use of MRI-based biomarkers in future preclinical trials as well as in human HD clinical trials.

Materials and methods

Animals and drug treatment

Transgenic N171-82Q HD mice were maintained by breeding heterozygous N171-82Q males with C3B6F1 females (Taconic). DNA was obtained from tails of the offspring for determination of the genotype and CAG repeat size by PCR assay which was performed by Laragen Inc (Los Angeles, CA, USA) genotyping service. The mice were housed in groups of 3–5 with access to food and water *ad libitum* and a 12-h light/dark cycle. Male mice with CAG repeat 82 used in this study were housed in cages that included an orange mouse igloo and a green nylabone. Sertraline (10 mg/kg, Toronto research Chemicals, Canada) was dissolved in 0.2% Tween-80 (vehicle) and administered at 6 weeks of age by i.p. injection daily. Age and gender-matched littermate wild type mice were used as controls. There were 15 mice in each group. All animal experiments were performed according to procedures approved by the Institutional Animal Care and Use Committee at the Johns Hopkins University.

In vivo MRI acquisition

In vivo studies were performed on a horizontal 9.4 Tesla MR scanner (Bruker Biospin, Billerica, MA, USA) with a triple-axis gradient and an animal imaging probe. The scanner was also equipped with a physiological monitoring system (EKG, respiration, and body temperature). Ten mice in each group were used in the MRI study, and 15 mice in each group were used for behavioral tests and survival curves. Mice were first scanned by MRI at 6 weeks of age, and scanning was repeated every 4 weeks after the first scan until 18 weeks. Mice were anesthetized with isoflurane (1%) together with oxygen and air at 1:3 ratios *via* a vaporizer and a facial mask. We used a 40-mm diameter birdcage coil for the radiofrequency transmitter and receiver. Temperature was maintained by a heating block built into the gradient system. Respiration was monitored throughout the entire scan. Images were acquired using a three-dimensional (3D) T2-weighted fast spin echo sequence, with the following parameters: echo time (TE)/repetition time (TR) = 40/700 ms, resolution = 0.1 mm × 0.1 mm × 0.25 mm, echo train length = 4, number of average = 2, and flip angle = 40°. The total imaging time was about 50 min per mouse. Mice recovered quickly once the anesthesia was turned off, and all 10 mice survived the repeated 50-min imaging sessions. Imaging resolution and contrast were sufficient for automatic volumetric characterization of mouse brain and substructures.

Image analysis

Initial processing

Images were first rigidly aligned to a template image by using automated image registration software (http://bishopw.loni.ucla.edu/AIR5/, AIR). The template image was selected from one of the images acquired from age-matched littermate control mice, which had been manually adjusted to the orientation defined by the Paxino's atlas with an isotropic resolution of 0.1 mm × 0.1 mm × 0.1 mm per pixel. After rigid alignment, images had the same position and orientation as the template image, and image resolution was also adjusted to an isotropic resolution of 0.1 mm × 0.1 mm × 0.1 mm per pixel. Signals from nonbrain tissue were removed manually (skull-stripping).

Computational analysis

Skull-stripped, rigidly aligned images were analyzed using the Diffeomap software (www.mristudio.org). Intensity values of the gray matter, white matter, and cerebral spinal fluid were normalized to the values in our MRI-based mouse brain atlas (Aggarwal et al., 2009) by using a piece-wise linear function. This procedure ensured that subject image and atlas image have similar intensity histograms. The intensity-normalized images were submitted by the Diffeomap software to a linux cluster, which runs Large Deformation Diffeomorphic Metric Mapping (LDDMM). The atlas consists of *in vivo* population averaged T2-weighted mouse brain image and segmentations of major gray and white matter structures (Aggarwal et al., 2009). Given images from different mouse brains, LDDMM automatically constructs nonlinear transformations between matching anatomical features on the basis of image intensity throughout the entire brain (Miller et al., 2002). The transformations deformed the structural segmentations in the atlas to the subject images to achieve automated segmentation of the subject images. The results of the automated segmentation were inspected and modified when necessary, and the volumes of each segmented structure were obtained. The transformations were also used for quantitative measurement of changes in local tissue volume among different mouse brains, by computing the Jacobian values of the transformations generated by

Please cite this article as: Cheng, Y., et al., Structural MRI detects progressive regional brain atrophy and neuroprotective effects in N171-82Q Huntington's disease mouse model, NeuroImage (2011), doi:10.1016/j.neuroimage.2011.02.022

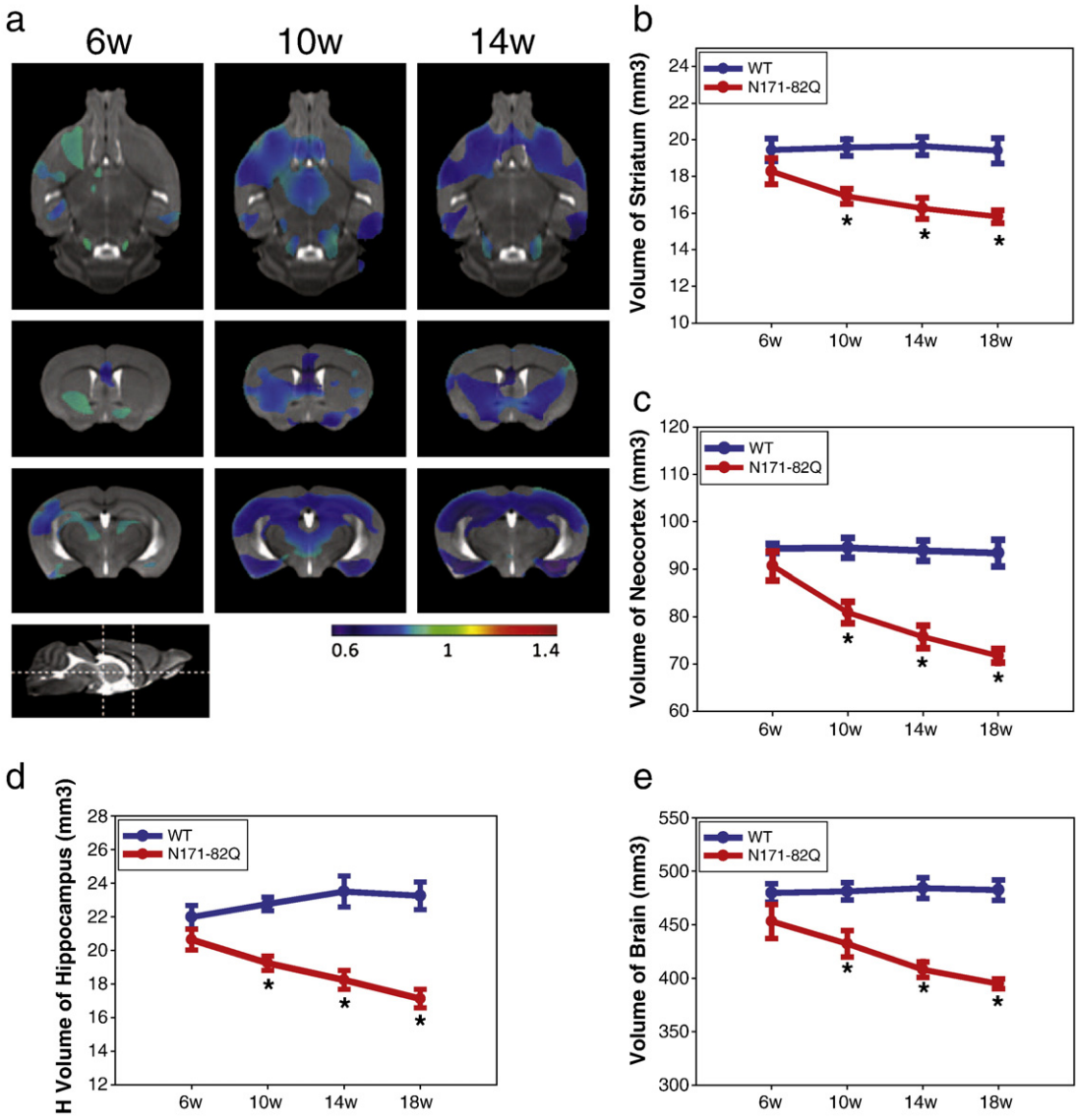

Fig. 1. Progressive brain atrophy detected by structural MRI in N171-82Q mouse model of Huntington's disease. (a) Regions of atrophy in the N171-82Q mouse brains detected by deformation-based morphometry (DBM) with respect to age- and gender-matched wild type (WT) littermate controls at 6, 10, and 14 weeks of age. Regions with significant atrophy (false discovery rate = 0.05) are highlighted in the reference mouse brain images and overlaid with the computed Jacobian values, which indicate the degree of local volume change. In the pseudo-color scheme dark green is used to indicate mild atrophy and blue or black indicates severe atrophy in the HD brains compared to age-matched controls. One horizontal and two coronal sections are shown (locations in the bottom scout image). (b–e) Progressive regional brain atrophy detected in striatum (b), neocortex (c), hippocampus (d) as well as whole brain (e). Mean ± SD; n = 15. *$p<0.05$ compared to the values of WT control mice. Two-way (genotype and age) repeated measurement analysis of variance was first performed to evaluate overall significance of changes in volumes. *Post-hoc* tests were performed using Student's *t*-tests with Bonferroni correction for multiple comparisons.

LDDMM. The advantage of LDDMM is that it generates accurate topology, preserving transformations between images. The transformations encode morphological differences between subject and template images and can be analyzed with deformation-based morphometry (DBM) (Ashburner and Friston, 2000) to detect regional changes in brain volumes. By combining MRI, LDDMM, and DBM, we can now investigate volumetric changes in the entire brain longitudinally without the need to explicitly define regions of interest.

Behavioral test and survival study

Mice were randomly divided into groups, each containing 15 mice. We used the same set of animals for survival analyses and motor performance tests. Survival was monitored daily by two experienced operators (Q. Peng and Y. Cheng). The mice were euthanized when HD mice were unable to right themselves after being placed on their backs and initiate movement after being gently prodded for 30 s. Motor behavioral performance was assessed with a rotarod apparatus (Columbus Instruments, OH) in which the time the mouse remains on the rod at accelerating speed from 4 to 40 rpm is measured. Each mouse was trained for 5 min and the training session was followed by a 1 h rest period in the home cage. Mice were then placed back on the rotarod for three trials of maximal 5 min at accelerating speeds (4–40 rpm) separated by a 30 min rest period. Mice were tested on 3 consecutive days, by which time a steady baseline level of performance was attained.

Statistics

Priori G*Power (version 3.1, Heinrich-Heine-University) analysis was used to calculate the necessary samples size and predict the feasibility by using changes in regional brain volumes as readout to evaluate the therapeutic effect in preclinical trials. The calculation was based on two sample independent *t*-tests ($\alpha = 0.05$, $\beta = 0.95$).

Please cite this article as: Cheng, Y., et al., Structural MRI detects progressive regional brain atrophy and neuroprotective effects in N171-82Q Huntington's disease mouse model, NeuroImage (2011), doi:10.1016/j.neuroimage.2011.02.022

Table 1
Regional brain volumes in N171-82Q mice compared to littermate controls.

Brain regions	WT (mm^3)	N171-82Q (mm^3)
Hypothalamus		
6 weeks	10.24 ± 0.53	9.97 ± 0.57
10 weeks	11.07 ± 0.40	9.69 ± 0.49*
14 weeks	11.14 ± 0.60	9.45 ± 0.46*
18 weeks	10.95 ± 0.68	9.05 ± 0.08*
Thalamus		
6 weeks	21.64 ± 0.79	20.15 ± 0.90
10 weeks	21.51 ± 0.45	18.55 ± 0.70*
14 weeks	21.50 ± 0.52	18.47 ± 0.38*
18 weeks	21.25 ± 0.63	18.12 ± 0.11*
Amygdala		
6 weeks	6.38 ± 0.25	6.03 ± 0.33
10 weeks	6.70 ± 0.37	5.59 ± 0.25*
14 weeks	6.85 ± 0.30	5.31 ± 0.21*
18 weeks	6.74 ± 0.37	5.14 ± 0.10*
Cerebellum		
6 weeks	61.00 ± 1.70	59.30 ± 3.30
10 weeks	60.50 ± 1.20	58.00 ± 2.60
14 weeks	61.60 ± 1.40	57.90 ± 2.40
18 weeks	60.50 ± 1.10	58.40 ± 2.50
Corpus callosum		
6 weeks	12.34 ± 0.60	10.76 ± 0.73*
10 weeks	12.79 ± 0.53	10.46 ± 0.67*
14 weeks	12.80 ± 0.57	10.28 ± 0.71*
18 weeks	12.71 ± 0.62	10.73 ± 0.61*

* $p<0.05$ compared to the values of age-matched wild type (WT) control mice.

Two-way (genotype and age) repeated measurement analysis of variance was performed to evaluate the overall significance of the changes in the volumes of the different brain regions as well as whole brain. *Post-hoc* tests were performed using Student's *t*-tests with Bonferroni correction for multiple comparisons. Statistical calculations were made using Sigmastat. Group comparison on the logarithm of the Jacobian values between N171-82Q HD mice and control mice or HD mice treated with sertraline and HD mice treated with vehicle at each age was performed at each pixel inside the brain by using one-way ANOVA with *posthoc* test with false discovery rate set at 0.05 to control for possible false positives (Genovese et al., 2002). Because the template image has orientation and position similar to that defined in Paxino's atlas, regions with significant atrophy were labeled according to the atlas. Survival data were analyzed by Kaplan–Meier analysis. Correlations between brain regional atrophy and motor behavioral performance were modeled using Pearsonian correlation analysis. Pearson coefficients were calculated from the slope.

Results

Adult-onset progressive brain atrophy is detected by longitudinal analysis of regional brain volumes in N171-82Q mice

We performed longitudinal *in vivo* structural MRI scans in 6-, 10-, 14-, and 18-week-old N171-82Q mice and their littermate controls to monitor the onset and progression of brain atrophy. N171-82Q HD mice exhibit adult-onset, progressive, and significant atrophy in the neocortex, striatum, hippocampus, hypothalamus, thalamus, and amygdala as well as in whole brain (Figs. 1a–e, Table 1). The cerebellum showed no significant volume change at all ages that we examined (Table 1). Interestingly, we also detected loss of white matter volume in the corpus callosum (Table 1) as early as 6 weeks of age. These findings are intriguing given recent reports in HD patients (Hobbs et al., 2010a,b; Nopoulos et al., 2010; Paulsen et al., 2010; Rosas et al., 2010), suggesting that white matter loss may be an early pathogenetic event and contribute to cortical–striatal disconnection and dysfunction. The results in the current study provided important information that enabled us to select appropriate age and brain

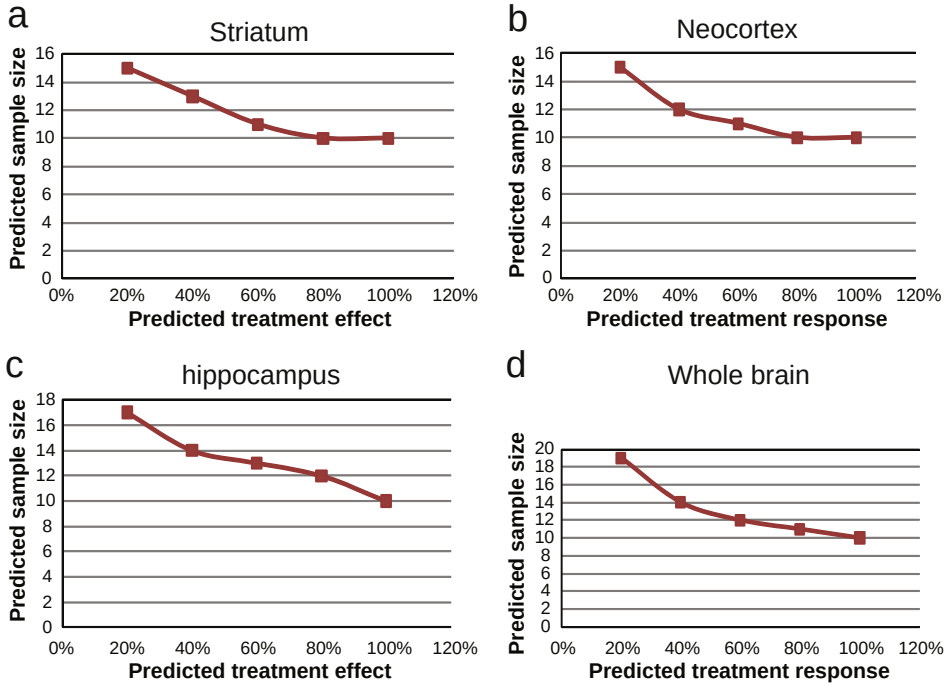

Fig. 2. Power analysis reveals that use of structural MRI is feasible for tracking disease progression and evaluating therapeutic response in N171-82Q HD model. Priori G*Power (version 3.1, Heinrich-Heine-University) analysis was used to calculate the necessary sample size by using volumes of striatum (a), neocortex (b), hippocampus (c), and whole brain (d) measured by structural MRI as outcome measures in preclinical trials. $\alpha = 0.05$, $\beta = 0.95$. The calculation is based on the mean and variability of differences in brain regional volumes between N171-82Q HD mice and their wild type littermate controls at 10 weeks of age. We set the volumetric differences in each brain region between untreated-HD mice and control mice at 100%, and used % improvement of brain atrophy as predicted treatment response to calculate the sample size for preclinical trials.

Please cite this article as: Cheng, Y., et al., Structural MRI detects progressive regional brain atrophy and neuroprotective effects in N171-82Q Huntington's disease mouse model, NeuroImage (2011), doi:10.1016/j.neuroimage.2011.02.022

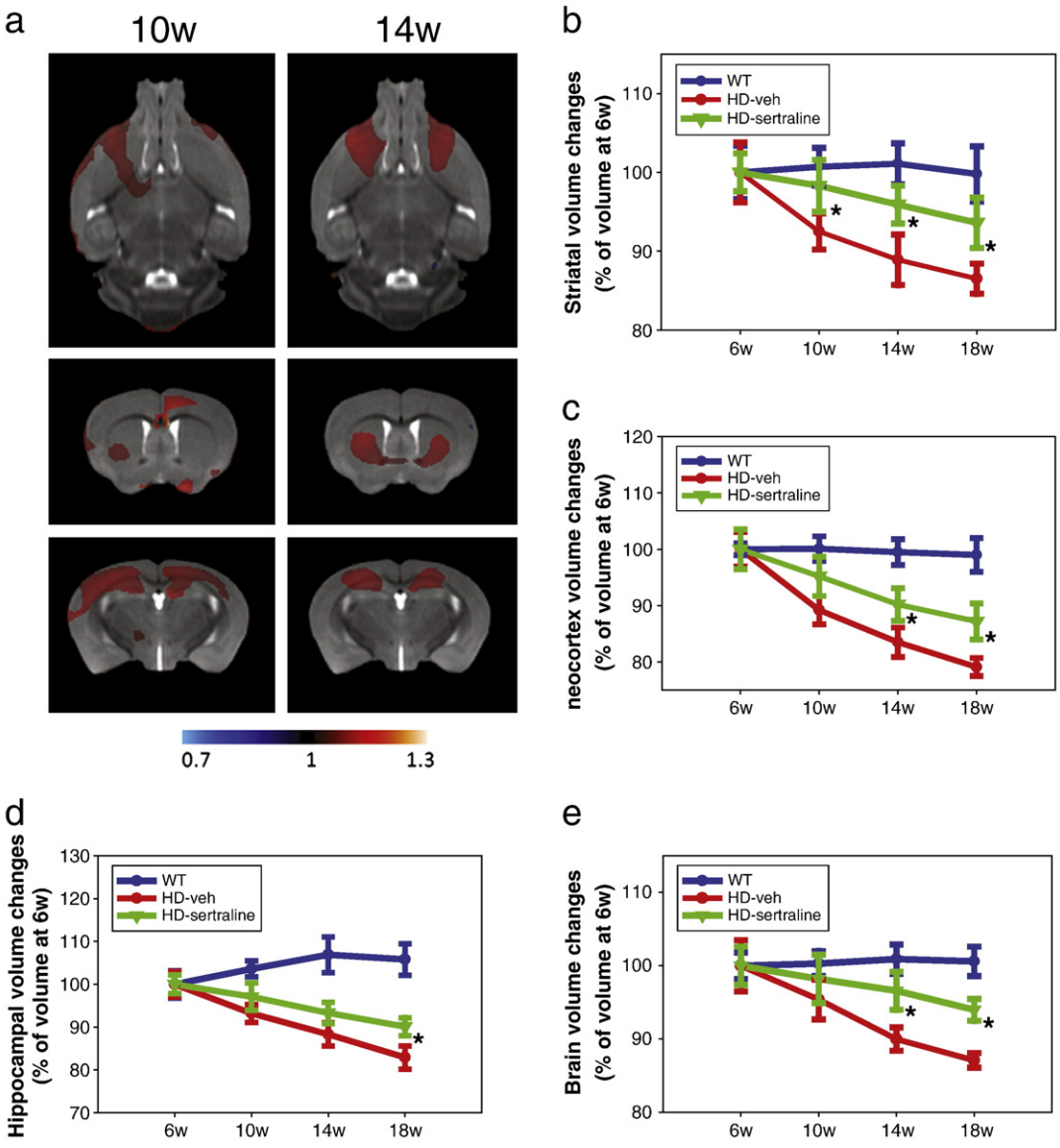

Fig. 3. Structural MRI detects therapeutic effect of neuroprotective treatment in N171-82Q HD mice. (a) Representative pictures indicate regions with significant local volumetric differences between sertraline- and vehicle-treated N171-82Q mice at 10 and 14 weeks of age. Regions with significant difference in the degree of atrophy between the treated and sham groups (false discovery rate = 0.05) are highlighted in the reference mouse brain images and overlaid with the computed Jacobian values, which indicate the degree of local volume difference. In the pseudo-color scheme orange and brown are used to indicate less severe atrophy and blue indicates more severe atrophy in the sertraline-treated HD brains compared to age-matched vehicle-treated controls. Horizontal and coronal sections are the same as those in Fig. 1. (b–e) Quantification of brain volume changes in striatum (b), neocortex (c), hippocampus (d), and whole brain (e) in sertraline-treated N171-82Q HD mice compared to vehicle-treated mice. Mean ± SD; n = 15 in each group. $^{*}p<0.05$ *vs* the values in vehicle treated HD mice. Two-way (genotype and age) repeated measurement analysis of variance was first performed to evaluate overall significance of changes in volumes. *Post-hoc* tests were performed using Student's *t*-tests with Bonferroni correction for multiple comparisons.

regional volume measures in N171-82Q HD mice for preclinical treatment evaluation. The findings also suggest that N171-82Q mice could be used for both presymptomatic and symptomatic preclinical trials.

Power analysis results of using structural MRI measures as outcome measures in preclinical trials

In order to determine the feasibility of using MRI measures as biomarkers for preclinical trials, we used Priori G*Power analysis (Version 3.1,) to predict the sample size for designing preclinical trials by using structural MRI measures as outcome readout. The calculation is based on the mean and variability of differences in brain regional volumes between N171-82Q HD mice and their wild type littermate controls at 10 weeks of age. We set the volumetric differences in each brain region between untreated HD mice and control mice at 100%, and used % improvement of brain atrophy as predicted treatment response to calculate the sample size for preclinical trials.

Our results indicate that 10–14 mice per group could provide 95% power to detect 40% improvement of brain atrophy by using volume changes of striatum, neocortex, and hippocampus, as well as whole brain as outcome measures (Figs. 2a–d); thus the power to detect therapeutic effects by MRI is feasible to be applied in preclinical trials.

MRI detects therapeutic response in N171-82Q mice

In order to determine whether structural MRI can detect treatment response, we administered sertraline, which was shown to be neuroprotective in N171-82Q mice in our previous study (Duan et al., 2008). Sertraline (10 mg/kg) was administered daily to mice starting at

Please cite this article as: Cheng, Y., et al., Structural MRI detects progressive regional brain atrophy and neuroprotective effects in N171-82Q Huntington's disease mouse model, NeuroImage (2011), doi:10.1016/j.neuroimage.2011.02.022

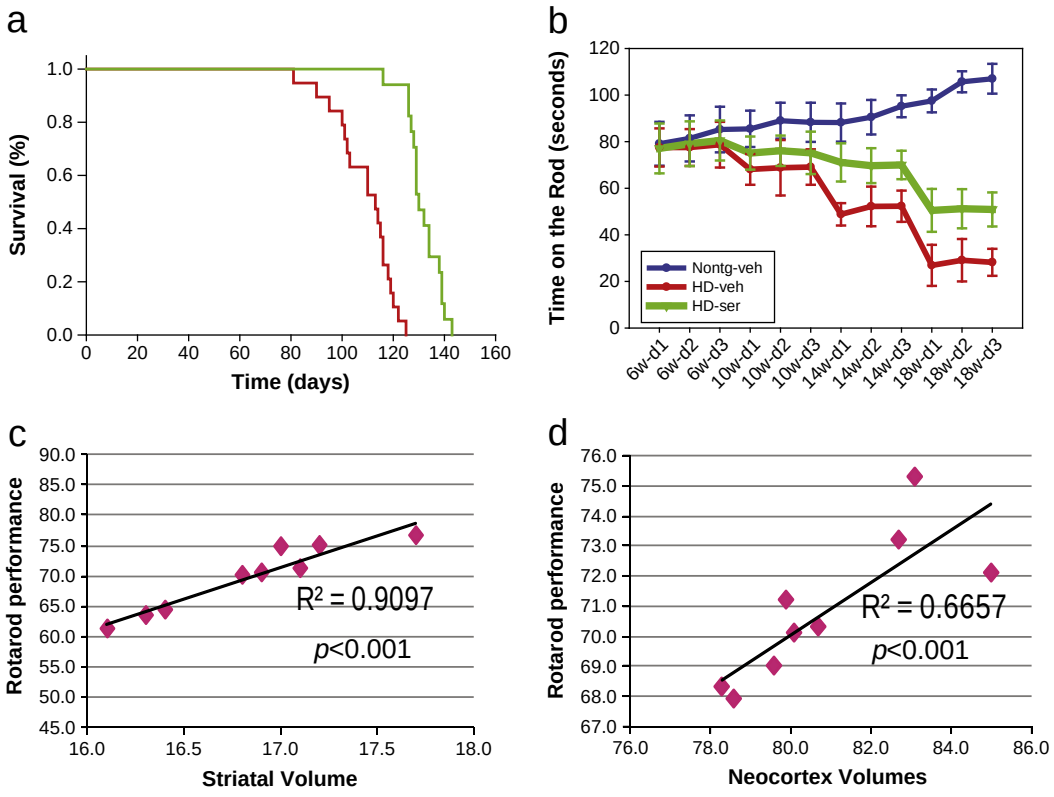

Fig. 4. Regional brain atrophy is correlated with motor dysfunction in N171-82Q mice. (a) Survival curve of HD mice treated with sertraline or vehicle. (b) Motor function was assessed by accelerating rotarod at indicated ages of HD mice and control mice. Mean ± SD; n = 15. (c) Correlation between striatal volume and rotarod performance. (d) Correlation between neocortex volume and motor performance.

6 weeks of age, and MRI scans were obtained at 6, 10, 14, and 18 weeks. MRI measures indicated that sertraline significantly slowed the rates of progression in regional brain atrophy in N171-82Q mice (Figs. 3a–e). Notably, striatal volume changes showed the most dramatic response to the sertraline treatment (Fig. 3b).

Correlation between atrophy in different brain regions and motor phenotype

The average survival time in the cohort of N171-82Q mice was 119 ± 2.4 days (mean ± SE, n = 19); sertraline treatment significantly increased average survival in treated mice to 139 ± 2.0 days (mean ± SE, n = 17, Fig. 4a). N171-82Q mice also demonstrated progressive motor deficits, which were slowed by sertraline treatment (Fig. 4b). In order to determine whether there is a correlation between brain volume loss and motor deficits in N171-82Q HD mice, we calculated correlations of volumes of different brain regions with measures of motor performance to validate the association between brain imaging and motor phenotype measures in these mice. The Pearson correlation coefficients for striatal volume and neocortex volume were significant for motor deficits (Figs. 4c–d). These results indicated that significant motor deficits, as evidenced by reduction of the time spent on the rotarod, were positively correlated with brain regional atrophy in striatum (Fig. 4c) and neocortex (Fig. 4d), but not with other brain regions such as cerebellum (data not shown).

Discussion

Although MRI has been used to evaluate brain atrophy and effects of treatment in HD mouse models, most studies were cross-sectional or only reported brain atrophy at one time point (Ferrante et al., 2000, 2002; Sawiak et al., 2009a,b). Compared to histology-based stereology, MRI is noninvasive, and it provides digitized data with full brain coverage, free from distortions due to embedding and sectioning. Longitudinal *in vivo* imaging of HD mice would allow a complete natural history of brain pathological changes to be developed during preclinical trials, and considerably increase the power to detect therapeutic efficacy compared to a single measurement of neuropathology. The current study of brain volumetric changes in a widely-used HD mouse model provides evidence that longitudinal structural MRI has the power to detect the response to neuroprotective treatment, suggesting that the N171-82Q mouse model is suitable for presymptomatic as well as symptomatic preclinical trials.

We also investigated correlations between the regional brain atrophy and motor dysfunction in N171-82Q HD mice. Progressive brain atrophy in striatum and cortex was positively correlated with deficits in motor function, suggesting that imaging measures could predict neuron functional changes. These results indicate that the functional change in N171-82Q mice may have originated from loss of brain volume. Interestingly, these HD mice exhibit dramatic motor deficits and short life-span, but subtle neurodegeneration. Our results suggest that motor phenotype in this mouse model may result from neuronal atrophy and dysfunction rather than neuronal loss; thus, neuroimaging measures might be ideal biomarkers for evaluation of neuroprotective treatment in preclinical trials.

Besides gray matter volume loss, we also detected loss of white matter volume at the early stage in N171-82Q mice. Clinical studies from HD patients' brains suggest two possible theories for decrease in white matter volume. For example, mutant huntingtin might have a direct effect on myelination such that, once myelinated, neuronal circuits become functional, myelin breakdown begins, which causes an excitotoxic process with failure of afferent transmissions causing the underlying neuron to be overstimulated by its efferent feedback (Gomez-Tortosa et al., 2001; Bartzokis et al., 2007). Alternatively, the deficit in white matter volume might be a manifestation of abnormal development instead of decreased volume from a degenerative

Please cite this article as: Cheng, Y., et al., Structural MRI detects progressive regional brain atrophy and neuroprotective effects in N171-82Q Huntington's disease mouse model, NeuroImage (2011), doi:10.1016/j.neuroimage.2011.02.022

process. Our data indicated earlier decreased white matter volume in the N171-82Q HD mice, but in contrast the volume loss is less progressive than loss of gray matter in these mice, suggesting that developmental defects might be involved in the white matter pathology in HD. Further detailed study of white matter at the earlier stage is needed.

In addition to conventional segmentation-based volume analysis, we have performed deformation-based morphometry (DBM) analysis based on the transformations generated by LDDMM to investigate potential brain atrophy in regions not easily definable, for example, the hypothalamus, and thalamus among others. DBM analysis has several advantages. It is free from intra-rater and inter-rater variations. It can be implemented in a fully automated fashion to increase throughput, which is often the bottleneck for therapeutic screening. It can locate and visualize localized atrophy, which is difficult to achieve with a segmentation-based approach (Maheswaran et al., 2009). The accuracy of the DBM approach, however, depends on the quality of the transformation and how concentrated the potential atrophy or hypertrophy is among animals (Davatzikos, 2004). For example, the complex geometry and relatively large morphological variations of the lateral ventricles in the mouse brain makes it challenging for LDDMM to generate accurate image transformations for the ventricles and neighboring regions (Zhang et al., 2010). The particular portion of the lateral ventricles that is enlarged might also be different among animals. As a result, DBM may not be able to detect volume changes near the lateral ventricles. The sensitivity of the DBM approach to detect atrophy or hypertrophy could also be lower than that of the segmentation-based volume analysis. The segmentation-based approach effectively averages the volume changes of a relatively large group of voxels and therefore has a much higher signal-to-noise ratio, whereas the DBM approach examines volume change at each voxel independently, with corrections for multiple comparisons.

In summary, longitudinal *in vivo* MRI allows us to investigate disease onset and progression over the life-span of each mouse, which will greatly facilitate preclinical therapeutic trials in HD mice. This approach will provide significant benefits for trials that use regional brain atrophy as an endpoint in treatment trials. These findings provide the first evidence of progressive brain volume loss in different brain regions of the N171-82Q HD mouse model in response to neuroprotective therapy. The findings also guarantee further characterization of other available HD mouse models and evaluation of therapeutics in preclinical trials by MRI.

Acknowledgments

We gratefully acknowledge Dr. Pamela Talalay for her dedicated editorial assistance. This research was supported by grant (CHDI A2120) from the CHDI Foundation, Inc. (to W. Duan), NINDS NS16375 (to CAR), NIH EB003543 and NIH ES012665 (to S. Mori), and NIH 65306 (to J. Zhang).

References

Aggarwal, M., Zhang, J., Miller, M.I., Sidman, R.L., Mori, S., 2009. Magnetic resonance imaging and micro-computed tomography combined atlas of developing and adult mouse brains for stereotaxic surgery. Neuroscience 162, 1339–1350.

Ashburner, J., Friston, K.J., 2000. Voxel-based morphometry—the methods. Neuroimage 11, 805–821.

Aylward, E.H., Codori, A.M., Rosenblatt, A., Sherr, M., Brandt, J., Stine, O.C., Barta, P.E., Pearlson, G.D., Ross, C.A., 2000. Rate of caudate atrophy in presymptomatic and symptomatic stages of Huntington's disease. Mov. Disord. 15, 552–560.

Aylward, E.H., Li, Q., Stine, O.C., Ranen, N., Sherr, M., Barta, P.E., Bylsma, F.W., Pearlson, G.D., Ross, C.A., 1997. Longitudinal change in basal ganglia volume in patients with Huntington's disease. Neurology 48, 394–399.

Aylward, E.H., Sparks, B.F., Field, K.M., Yallapragada, V., Shpritz, B.D., Rosenblatt, A., Brandt, J., Gourley, L.M., Liang, K., Zhou, H., Margolis, R.L., Ross, C.A., 2004. Onset and rate of striatal atrophy in preclinical Huntington disease. Neurology 63, 66–72.

Bartzokis, G., Lu, P.H., Tishler, T.A., Fong, S.M., Oluwadara, B., Finn, J.P., Huang, D., Bordelon, Y., Mintz, J., Perlman, S., 2007. Myelin breakdown and iron changes in Huntington's disease: pathogenesis and treatment implications. Neurochem. Res. 32, 1655–1664.

Ciarmiello, A., Cannella, M., Lastoria, S., Simonelli, M., Frati, L., Rubinsztein, D.C., Squitieri, F., 2006. Brain white-matter volume loss and glucose hypometabolism precede the clinical symptoms of Huntington's disease. J. Nucl. Med. 47, 215–222.

Davatzikos, C., 2004. Why voxel-based morphometric analysis should be used with great caution when characterizing group differences. Neuroimage 23, 17–20.

Duan, W., Peng, Q., Masuda, N., Ford, E., Tryggestad, E., Ladenheim, B., Zhao, M., Cadet, J.L., Wong, J., Ross, C.A., 2008. Sertraline slows disease progression and increases neurogenesis in N171-82Q mouse model of Huntington's disease. Neurobiol. Dis. 30, 312–322.

Ferrante, R.J., Andreassen, O.A., Dedeoglu, A., Ferrante, K.L., Jenkins, B.G., Hersch, S.M., Beal, M.F., 2002. Therapeutic effects of coenzyme Q10 and remacemide in transgenic mouse models of Huntington's disease. J. Neurosci. 22, 1592–1599.

Ferrante, R.J., Andreassen, O.A., Jenkins, B.G., Dedeoglu, A., Kuemmerle, S., Kubilus, J.K., Kaddurah-Daouk, R., Hersch, S.M., Beal, M.F., 2000. Neuroprotective effects of creatine in a transgenic mouse model of Huntington's disease. J. Neurosci. 20, 4389–4397.

Genovese, C.R., Lazar, N.A., Nichols, T., 2002. Thresholding of statistical maps in functional neuroimaging using the false discovery rate. Neuroimage 15, 870–878.

Gomez-Tortosa, E., MacDonald, M.E., Friend, J.C., Taylor, S.A., Weiler, L.J., Cupples, L.A., Srinidhi, J., Gusella, J.F., Bird, E.D., Vonsattel, J.P., Myers, R.H., 2001. Quantitative neuropathological changes in presymptomatic Huntington's disease. Ann. Neurol. 49, 29–34.

Halliday, G.M., McRitchie, D.A., Macdonald, V., Double, K.L., Trent, R.J., McCusker, E., 1998. Regional specificity of brain atrophy in Huntington's disease. Exp. Neurol. 154, 663–672.

Harris, G.J., Aylward, E.H., Peyser, C.E., Pearlson, G.D., Brandt, J., Roberts-Twillie, J.V., Barta, P.E., Folstein, S.E., 1996. Single photon emission computed tomographic blood flow and magnetic resonance volume imaging of basal ganglia in Huntington's disease. Arch. Neurol. 53, 316–324.

Harris, G.J., Codori, A.M., Lewis, R.F., Schmidt, E., Bedi, A., Brandt, J., 1999. Reduced basal ganglia blood flow and volume in pre-symptomatic, gene-tested persons at-risk for Huntington's disease. Brain 122 (Pt 9), 1667–1678.

Harris, G.J., Pearlson, G.D., Peyser, C.E., Aylward, E.H., Roberts, J., Barta, P.E., Chase, G.A., Folstein, S.E., 1992. Putamen volume reduction on magnetic resonance imaging exceeds caudate changes in mild Huntington's disease. Ann. Neurol. 31, 69–75.

Hobbs, N.Z., Barnes, J., Frost, C., Henley, S.M., Wild, E.J., Macdonald, K., Barker, R.A., Scahill, R.I., Fox, N.C., Tabrizi, S.J., 2010a. Onset and progression of pathologic atrophy in Huntington disease: a longitudinal MR imaging study. AJNR Am J Neuroradiol. 31, 1036–1041.

Hobbs, N.Z., Henley, S.M., Ridgway, G.R., Wild, E.J., Barker, R.A., Scahill, R.I., Barnes, J., Fox, N.C., Tabrizi, S.J., 2010b. The progression of regional atrophy in premanifest and early Huntington's disease: a longitudinal voxel-based morphometry study. J. Neurol. Neurosurg. Psychiatry 81, 756–763.

Kassubek, J., Bernhard Landwehrmeyer, G., Ecker, D., Juengling, F.D., Muche, R., Schuller, S., Weindl, A., Peinemann, A., 2004. Global cerebral atrophy in early stages of Huntington's disease: quantitative MRI study. NeuroReport 15, 363–365.

Kloppel, S., Henley, S.M., Hobbs, N.Z., Wolf, R.C., Kassubek, J., Tabrizi, S.J., Frackowiak, R.S., 2009. Magnetic resonance imaging of Huntington's disease: preparing for clinical trials. Neuroscience 164, 205–219.

Maheswaran, S., Barjat, H., Bate, S.T., Aljabar, P., Hill, D.L., Tilling, L., Upton, N., James, M.F., Hajnal, J.V., Rueckert, D., 2009. Analysis of serial magnetic resonance images of mouse brains using image registration. Neuroimage 44, 692–700.

Miller, M.I., Trouve, A., Younes, L., 2002. On the metrics and Euler–Lagrange equations of computational anatomy. Annu. Rev. Biomed. Eng. 4, 375–405.

Nopoulos, P.C., Aylward, E.H., Ross, C.A., Johnson, H.J., Magnotta, V.A., Juhl, A.R., Pierson, R.K., Mills, J., Langbehn, D.R., Paulsen, J.S., 2010. Cerebral cortex structure in prodromal Huntington disease. Neurobiol. Dis. 40, 544–554.

Paulsen, J.S., Langbehn, D.R., Stout, J.C., Aylward, E., Ross, C.A., Nance, M., Guttman, M., Johnson, S., MacDonald, M., Beglinger, L.J., Duff, K., Kayson, E., Biglan, K., Shoulson, I., Oakes, D., Hayden, M., 2008. Detection of Huntington's disease decades before diagnosis: the Predict-HD study. J. Neurol. Neurosurg. Psychiatry 79, 874–880.

Paulsen, J.S., Magnotta, V.A., Mikos, A.E., Paulson, H.L., Penziner, E., Andreasen, N.C., Nopoulos, P.C., 2006. Brain structure in preclinical Huntington's disease. Biol. Psychiatry 59, 57–63.

Paulsen, J.S., Nopoulos, P.C., Aylward, E., Ross, C.A., Johnson, H., Magnotta, V.A., Juhl, A., Pierson, R.K., Mills, J., Langbehn, D., Nance, M., 2010. Striatal and white matter predictors of estimated diagnosis for Huntington disease. Brain Res. Bull. 82, 201–207.

Peng, Q., Masuda, N., Jiang, M., Li, Q., Zhao, M., Ross, C.A., Duan, W., 2008. The antidepressant sertraline improves the phenotype, promotes neurogenesis and increases BDNF levels in the R6/2 Huntington's disease mouse model. Exp. Neurol. 210, 154–163.

Reading, S.A., Yassa, M.A., Bakker, A., Dziorny, A.C., Gourley, L.M., Yallapragada, V., Rosenblatt, A., Margolis, R.L., Aylward, E.H., Brandt, J., Mori, S., van Zijl, P., Bassett, S.S., Ross, C.A., 2005. Regional white matter change in pre-symptomatic Huntington's disease: a diffusion tensor imaging study. Psychiatry Res. 140, 55–62.

Rosas, H.D., Goodman, J., Chen, Y.I., Jenkins, B.G., Kennedy, D.N., Makris, N., Patti, M., Seidman, L.J., Beal, M.F., Koroshetz, W.J., 2001. Striatal volume loss in HD as measured by MRI and the influence of CAG repeat. Neurology 57, 1025–1028.

Rosas, H.D., Lee, S.Y., Bender, A.C., Zaleta, A.K., Vangel, M., Yu, P., Fischl, B., Pappu, V., Onorato, C., Cha, J.H., Salat, D.H., Hersch, S.M., 2010. Altered white matter microstructure in the corpus callosum in Huntington's disease: implications for cortical "disconnection". Neuroimage 49, 2995–3004.

Rosas, H.D., Tuch, D.S., Hevelone, N.D., Zaleta, A.K., Vangel, M., Hersch, S.M., Salat, D.H., 2006. Diffusion tensor imaging in presymptomatic and early Huntington's disease:

Please cite this article as: Cheng, Y., et al., Structural MRI detects progressive regional brain atrophy and neuroprotective effects in N171-82Q Huntington's disease mouse model, NeuroImage (2011), doi:10.1016/j.neuroimage.2011.02.022

selective white matter pathology and its relationship to clinical measures. Mov. Disord. 21, 1317–1325.
Sawiak, S.J., Wood, N.I., Williams, G.B., Morton, A.J., Carpenter, T.A., 2009a. Use of magnetic resonance imaging for anatomical phenotyping of the R6/2 mouse model of Huntington's disease. Neurobiol. Dis. 33, 12–19.
Sawiak, S.J., Wood, N.I., Williams, G.B., Morton, A.J., Carpenter, T.A., 2009b. Voxel-based morphometry in the R6/2 transgenic mouse reveals differences between genotypes not seen with manual 2D morphometry. Neurobiol. Dis. 33, 20–27.
Tabrizi, S.J., Langbehn, D.R., Leavitt, B.R., Roos, R.A., Durr, A., Craufurd, D., Kennard, C., Hicks, S.L., Fox, N.C., Scahill, R.I., Borowsky, B., Tobin, A.J., Rosas, H.D., Johnson, H., Reilmann, R., Landwehrmeyer, B., Stout, J.C., 2009. Biological and clinical manifestations of Huntington's disease in the longitudinal TRACK-HD study: cross-sectional analysis of baseline data. Lancet Neurol. 8, 791–801.
Wild, E.J., Henley, S.M., Hobbs, N.Z., Frost, C., MacManus, D.G., Barker, R.A., Fox, N.C., Tabrizi, S.J., 2010. Rate and acceleration of whole-brain atrophy in premanifest and early Huntington's disease. Mov. Disord. 25, 888–895.
Zhang, J., Peng, Q., Li, Q., Jahanshad, N., Hou, Z., Jiang, M., Masuda, N., Langbehn, D.R., Miller, M.I., Mori, S., Ross, C.A., Duan, W., 2010. Longitudinal characterization of brain atrophy of a Huntington's disease mouse model by automated morphological analyses of magnetic resonance images. Neuroimage 49, 2340–2351.

Please cite this article as: Cheng, Y., et al., Structural MRI detects progressive regional brain atrophy and neuroprotective effects in N171-82Q Huntington's disease mouse model, NeuroImage (2011), doi:10.1016/j.neuroimage.2011.02.022